

STRUCTURAL CHARACTERIZATION OF NIOBIUM FILMS DEPOSITED BY ECR PLASMA ENERGETIC CONDENSATION ON CRYSTALLINE INSULATORS*

Xin Zhao^{1, #}, A.-M. Valente-Feliciano¹, J.K. Spradlin¹, H.L. Phillips¹, C.E. Reece¹,
D. Gu², H. Baumgart², K. Seo³

¹ Jefferson Lab, Newport News, VA, U.S.A.

² Old Dominion University, Norfolk, VA, U.S.A.

³ Norfolk State University, Norfolk, VA, U.S.A.

Abstract

An energetic condensation thin film coating technique with an electron cyclotron resonance (ECR) induced Niobium (Nb) plasma ion source is used to deposit Nb thin films on crystalline insulating substrates, such as *a*-plane and *c*-plane sapphire (Al₂O₃) and on magnesium oxide, MgO (100), (110), and (111).

Hetero-epitaxial Nb films were produced by ECR deposition with regulated substrate temperature. The residual resistivity ratio (RRR) of about 1 micron thick films on *a*-plane (1,1,-2,0) sapphire substrates reach values (350 - 450) comparable to high RRR bulk Nb commonly used for SRF cavities.

The epitaxial relationship of Nb/crystalline substrate is found to be strongly influenced by the substrate bias voltage (added to the initial Nb⁺ kinetic energy, 64 eV), the substrate crystalline orientation, and heating conditions.

At low substrate temperature, the Nb films demonstrate crystalline textures, revealed by XRD Pole Figure technique and Electron Backscattering Diffraction (EBSD). Niobium, as most metals, is known to grow with the "Volmer-Weber" growth mode, i.e. island growth.

This study shows that the film's crystal structural character has great impact on its RRR/T_c values.

INTRODUCTION

The characterization of the microstructure of ECR Niobium (Nb) thin films on crystalline insulator materials is practical in many interdisciplinary fields. For instance, sapphire is a well-known substrate to investigate Nb epitaxial growth. For Superconducting Radio-Frequency (SRF) particle accelerators, Nb and Nb compound thin films inter-layered with a dielectric buffer layer (such as a 50 nm layer of Al₂O₃ to suppress vortex-induced breakdown) might be a promising approach to replace the state-of-the-art bulk Nb materials in order to achieve higher accelerating gradient and to reduce liquid He cryogenic expense [1].

* Authored by Jefferson Science Associates, LLC under U.S. DOE Contract No. DE-AC05-06OR23177. The U.S. Government retains a non-exclusive, paid-up, irrevocable, world-wide license to publish or reproduce this manuscript for U.S. Government purposes.

[#]xinzhao@jlab.org

METHODS

In this study, an energetic condensation thin film coating technique, known as Electron Cyclotron Resonance (ECR), is applied to deposit Nb thin films on a variety of crystalline insulating substrates, such as *a*-plane (11-20) and *c*-plane (0001) sapphire (Al₂O₃) and on magnesium oxide, MgO (100). By controlling the coating time, thickness of all the films in this study is about 1 micron.

The crystal structure and texture were investigated via X-ray diffraction (XRD) $\theta/2\theta$ and pole figure scans with a four-circle PANalytical X'Pert PRO-MRD diffractometer. The diffractometer scanned over a 2θ range from 30° to 120° at step size 0.02°. The slit aperture of the X-ray source is 10×17mm. The scan has a divergence slit of 0.5°, a receiving slit of 0.1° and use a line focus Mirror primary optics with Cu *K* α source. The source with wavelength λ_{Cu} =1.54 Å was operated at 45 kV and 40 mA. XRD Pole Figures in Stereographic Projection format were used to investigate the "texture" (grains distribution in-plane) [2]. Pole figure (or texture) measurement is an efficient way to reveal polycrystalline structural character in a material.

Electron-beam backscattering diffraction (EBSD) characterization of the samples was conducted using a state-of-the-art TSL/EDAX OIMTM system. EBSD relies on rastering the e-beam of a scanning electron microscope (SEM) and/or moving the sample stage to map a large area. The uniqueness of this technique is being able to probe the crystal orientation of a small domain (tens of nanometers). The OIMTM software can automatically interpret the domain's crystal orientation by indexing the Kikuchi-bands diffraction pattern. The crystal orientations of the scanning points are rendered by a color map, called the Inverse Pole Figure (IPF). For instance, a pixel in green means the domain has a {110} orientation in-plane.

In this study, the grayscale of all the IPFs is rendered by the *Confidence Index* (C.I.). Dark and gray pixels are the points of low confidence indexes (CI < 0.05). Although there is no quantified relationship between crystalline order and CI, qualitatively, lower CI suggests lower crystallinity. The black or deep gray areas in an IPF color map might be the zones where either the grain size is <50nm or the grains might be entirely amorphous. The Kikuchi-diffraction patterns from these low CI zones were observed to be very faint or could not be indexed by the OIMTM software.

In order to discriminate within the {110} family (because all {110} orientations are rendered in green), the OIM™ software can plot raw data in a view of pole figure to visualize the texture. Compared to the XRD’s probing depth of 1-2 microns, EBSD probes only the top most surface (~50nm). Pole figures generated by both EBSD and XRD are complementary tools to reveal the reciprocal lattice (structural properties) of materials.

The method of RRR (R_{300K}/R_{10K}) and T_c measurement in this study was reported previously [3]. The four-point-probe test fixtures can measure resistivity of the Nb thin films from 300K and 4K.

RESULTS & DISCUSSION

Nb Thin Films on a-plane Sapphire

Single crystal sapphire has the *hexagonal-close-packed* (hcp) crystal structure, Al_2O_3 . The *a*-plane (11-20) and *c*-plane (0001) Al_2O_3 substrates, provided by INSACO™, have a $5 \times 20 \text{ mm}^2$ surface area and a 0.5° miscut. Before and during deposition, the substrate heating temperature is regulated. A constant bias potential is applied to the substrates during deposition.

Table 1a (plotted in Figure 1a shows the values of RRR and EBSD average CI, for samples coated at different bias voltages. The substrate baking and heating temperatures were both set at $360^\circ C$.

Table 1b (plotted in Figure 1b) presents the RRR and EBSD CI, for films coated at $-120V$ with various substrate heating parameters.

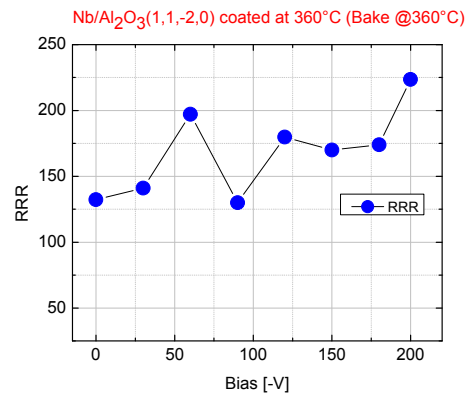
EBSD and XRD measurements found that all the samples have Nb {110} *in-plane* orientation (parallel to the substrate surface).

Table 1: (a) By fixing heating temperature (at $360^\circ C/360^\circ C$), RRR, EBSD CIs versus deposition bias. (b) By fixing bias voltage, RRR, EBSD CIs versus heating parameters for $-120V$ bias.

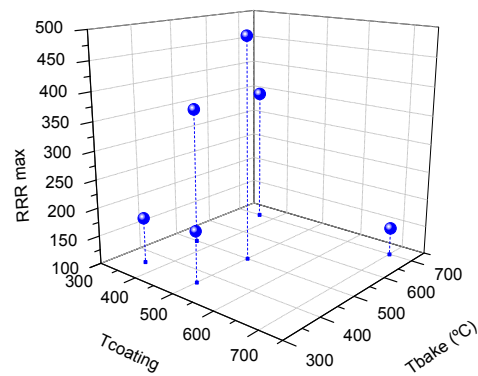
Deposition Bias (-Volts)	RRR	Avg. CI	Substrate Preparation Heat-Treatment ($^\circ C$)	Deposition Temp. ($^\circ C$)	RRR	EBSD Avg. C.I.
0	132	0.72				
30	141	0.72				
60	197	0.79	$360^\circ C$	$360^\circ C$	180	0.62
90	130	0.58	$360^\circ C$	$500^\circ C$	189	0.77
120	180	0.62	$700^\circ C$	$360^\circ C$	348	0.82
150	170	0.58	$500^\circ C$	$360^\circ C$	348	0.82
200	224	n/a	$500^\circ C$	$500^\circ C$	488	0.77

(a)

(b)



(a)



(b)

Figure 1: (a) RRR vs. Bias (plot of Table 1a); (b) RRR vs. Bias (plot of Table 1b).

Figure 2 is a XRD $\theta/2\theta$ survey of a Nb/*a*-sapphire film, coated at $500^\circ C/500^\circ C$ and $-120V$ bias. This sample yields the highest RR value (488) in the considered set of samples. The $\theta/2\theta$ survey demonstrates the presence of only Nb{110} orientation(s) in-plane.

Figure 3 represents the EBSD map and Inverse Pole Figure (IPF) for the same sample (a, b) with a color-mapped IPF for reference(c). The EBSD IPFs reveal the same Nb{110} *in-plane* structure as XRD.

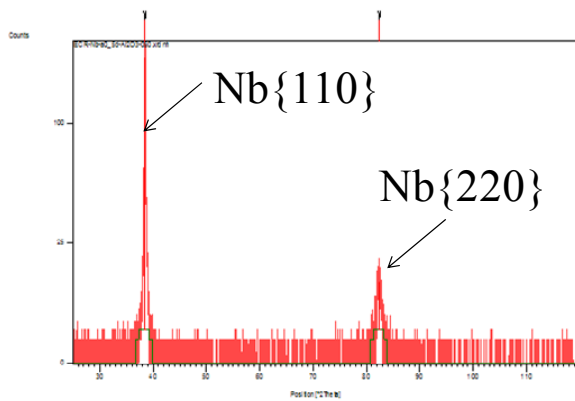


Figure 2: XRD $\theta/2\theta$ Survey of a Nb/*a*-sapphire, which was coated at 500°C/500°C, -120V bias.

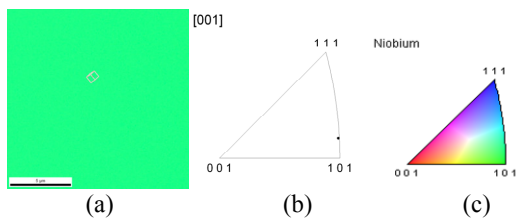


Figure 3: EBSD Map (a), IPF (b) of the same sample, as for Figure 2, reference color-mapped IPF(c).

The $\{110\}$ pole figure of an ideal single crystal Nb is plotted in Figure 4a (the inset of a green frame-box at top right represents the orientation of a *bcc* lattice). In the mock-up PF, the red dots represent the seven Nb $\{110\}$ planes in one single crystal lattice. Figure 4b is the pole figure plotted by the OIM™ software, based on the exact raw data for figure 3. The 7-dots pattern of the EBSD (110) pole figure (at top-right quadrant of 4b) demonstrated that no visible texture in the sample (500°C/500°C, -120V bias). In other words, it has the structure of a Nb $\{110\}$ single crystal laying on *a*-plane, Al₂O₃(11-20) plane.

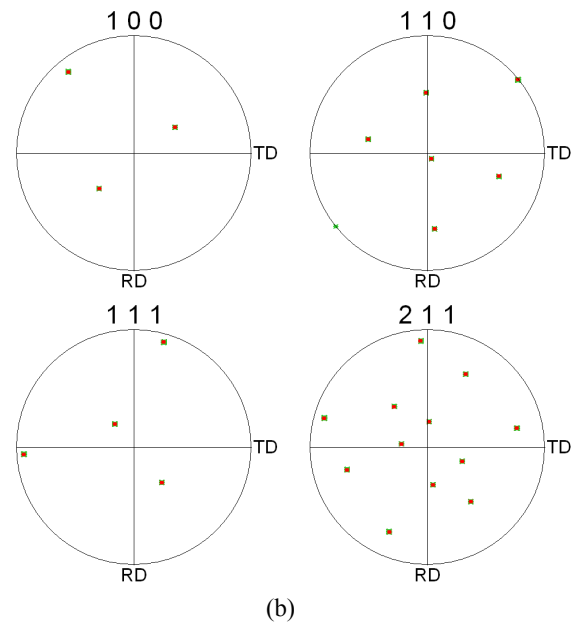
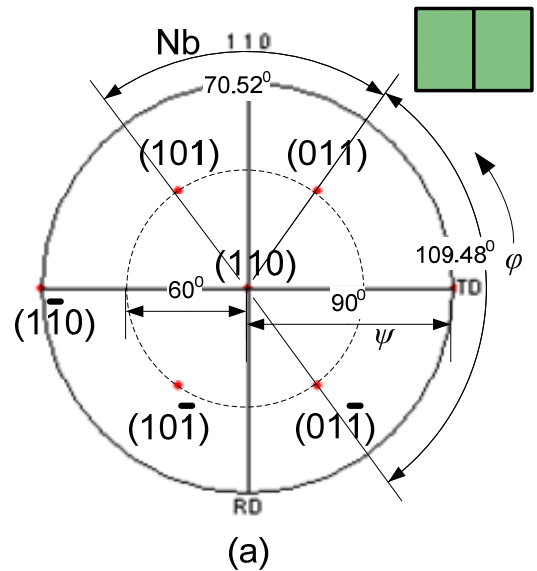


Figure 4: (a) $\{110\}$ pole figure of a body-centered cubic system, e.g. an ideal single crystal Nb. (b) EBSD pole figures of the sample (500°C/500°C, -120V bias).

The epitaxy of Nb/sapphire coating depends on a specific crystal plane. According to Wildes [4], Claassen *et al* [5, 6], Nb/Al₂O₃ epitaxial orientation is a special “Three-Dimensional (3D) Registry between the two (crystal) lattices”. Figure 5 (from Wildes’ review) represents the Nb/Al₂O₃ epitaxial relationships. The sapphire lattice below the Nb film “constrains” the alignment (orientation) of the Nb lattice above it. On *a*-plane, the reported epitaxial relationship is Nb $\{110\}$ ||Al₂O₃{1,1,-2,0}. Our XRD and EBSD measurements (Figure 2-4) verify this convention.

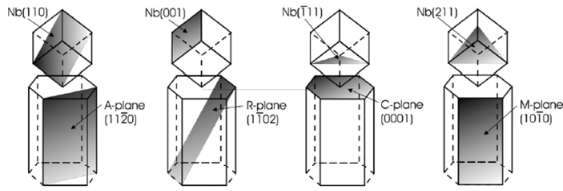


Figure 5: Crystal structure and planes of sapphire, Al_2O_3 . Three-dimensional epitaxial relationship proposed by Wildes, Claassen, et al [3].

Nb Thin Films on c-plane Sapphire

In this series, *c*-plane single crystal sapphire, Al_2O_3 (0001) with a 0.5° miscut is used as the coating substrate. All the samples were prepared by heating at 360°C , then coated at 360°C . Table 2 shows the samples' RRR, EBSD CIs and in-plane orientation, for different bias voltages. Our experiments discovered that the single-crystal-like Nb/*c*-sapphire films have different epitaxial relationships, depending on bias. For bias $< -90\text{V}$, the films have a Nb(111) orientation in-plane. At a higher bias, the films have a Nb(110) orientation. This was previously observed for MBE (molecular beam epitaxy) Nb films coated at 900°C and 1100°C [7].

Table 2: Nb/*c*-sapphire samples' RRR, EBSD CI and *in-plane* orientation (extracted from EBSD data), depending on different bias voltages. All samples were deposited with bake and coating temperatures of 360°C .

Deposition Bias (-Volts)	RRR	Avg. CI	In-plane Orientation
0	84	0.82	Nb(111)
60	108	0.64	Nb(111)
90	98	0.74	Nb(111)
120	54	0.11	Nb(110)
150	190	0.82	Nb(110)
200	99	n/a	Nb(110)

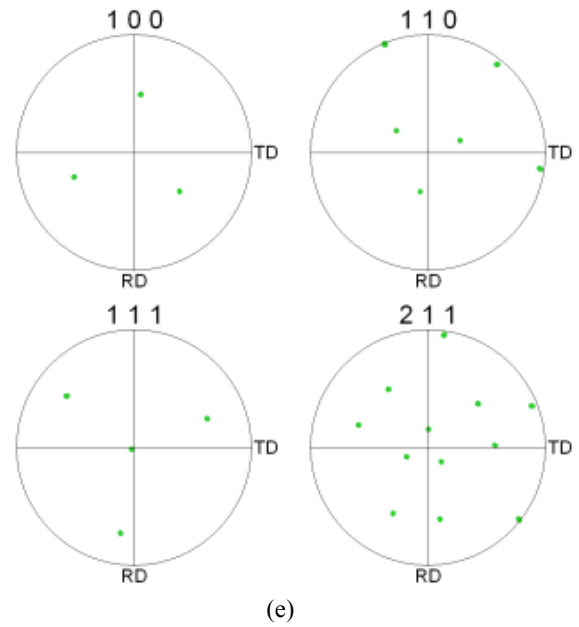
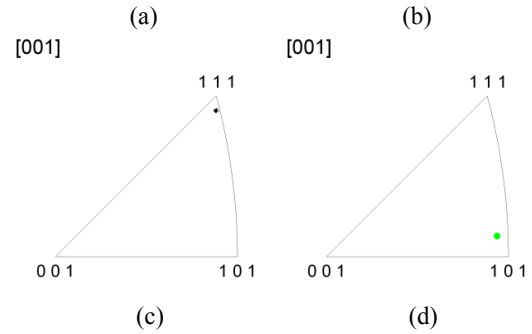
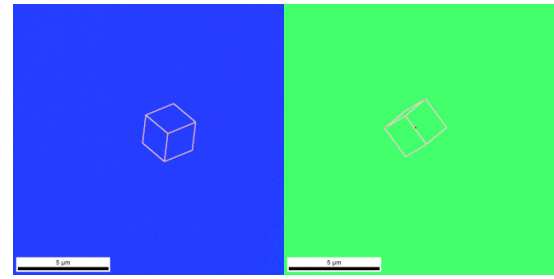
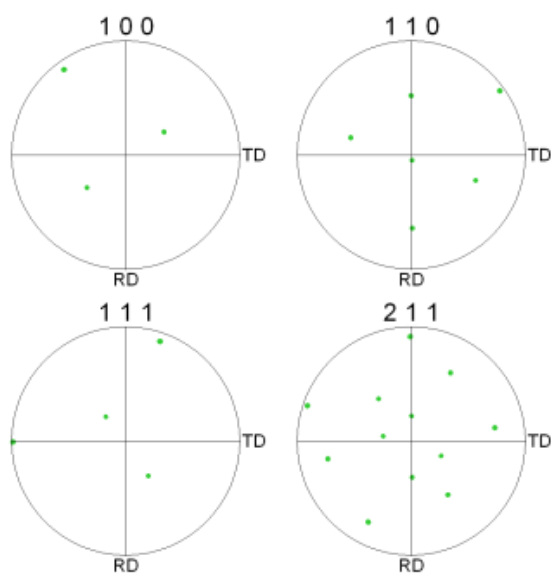


Figure 6 represents the EBSD data for Nb/*c*-sapphire film coated at $360^\circ\text{C}/360^\circ\text{C}$ and respectively (a, c, e) 0V bias (Row 1 in Table 2) and (b, d, f) -150V bias (Row 5 in Table 2).

The EBSD IPFs indicate a Nb{111} orientation for 0V bias (figure 6a,c) and a Nb{110} orientation (figure 6b, d) Both samples (figure e, f) are confirmed to be single crystals.



(f)

Figure 6: EBSD survey of two Nb/c-plane Al₂O₃ samples coated at 360°C/360°C for (a, c, e) 0V bias and (b, d, f) for -150V.

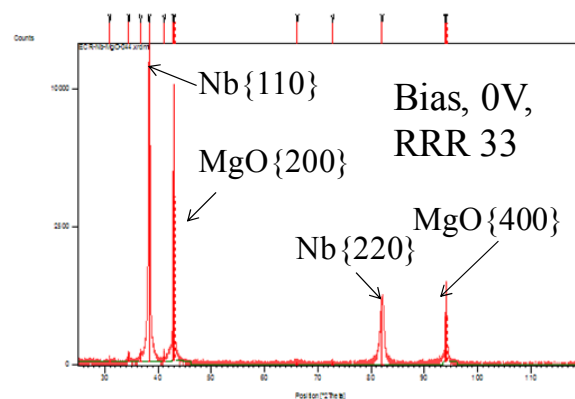
Nb Thin Films on Magnesium Oxide, MgO(100)

Single crystal Magnesium oxide has a *face-centered-cubic* (fcc) crystal structure. The samples, provided by MTI™, have a surface area of 10×10 mm². The MgO(100) crystal plane is used as coating substrate. In this series, all the substrates were baked and coated at 360°C. Table 3 shows the samples' RRR, EBSD CI for different bias voltages. For all the samples, XRD and EBSD survey found only Nb {110} orientation(s) in-plane.

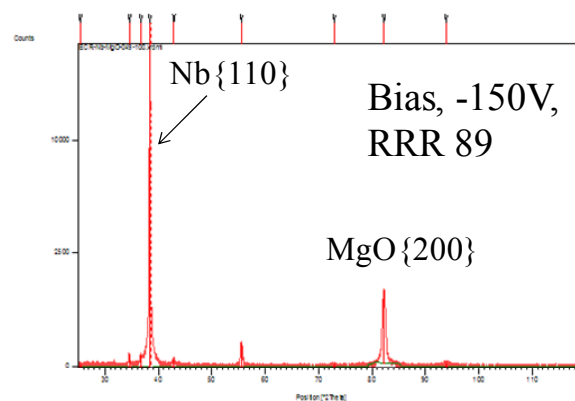
Table 3: RRR values versus deposition bias. The substrate baking and heating are 360°C.

Deposit ion Bias (-Volts)	RRR	Avg. CI.
0	33	0.08
30	51	0.28
60	59	0.1
90	58	0.1
120	81	0.42
150	89	0.38
200	82	n/a

Figure 7 is the XRD $\theta/2\theta$ survey of two Nb (110)/MgO(100) films coated at (a) 0V bias (Row 1 in Table 3) and (b) -150V bias (Row 6 in Table 2). Both figures endorse that only Nb{110} orientation(s) *in-plane* are present.



(a)



(b)

Figure 7: XRD $\theta/2\theta$ Survey of two Nb/MgO(110) films. (a) is of a sample coated with 0V bias, (b) is of -150V bias.

Figure 8 represents the EBSD survey of Nb/MgO(100) films coated at 360°C/360°C and (a, c) 0V bias (Row 1 in Table 3) and (b, d)-150V bias (Row 6 in Table 3).

The EBSD IPF (Figure 8a) shows for 0V bias a Nb{110} orientation (rendered in green). This color map has a multitude of dark pixels identifying the low CI areas. This suggests that on top-most surface (~50nm), there exists areas of grain size <50nm, amorphous structure or having a high density of structural defects (voids, dislocations). The corresponding EBSD pole figure (Figure 8c), confirms that the film is not a single crystal.

Figure 8(b d) indicates a single Nb{110} orientation (rendered in green). The XRD data from Figure 7b confirm that the film is a single crystal.

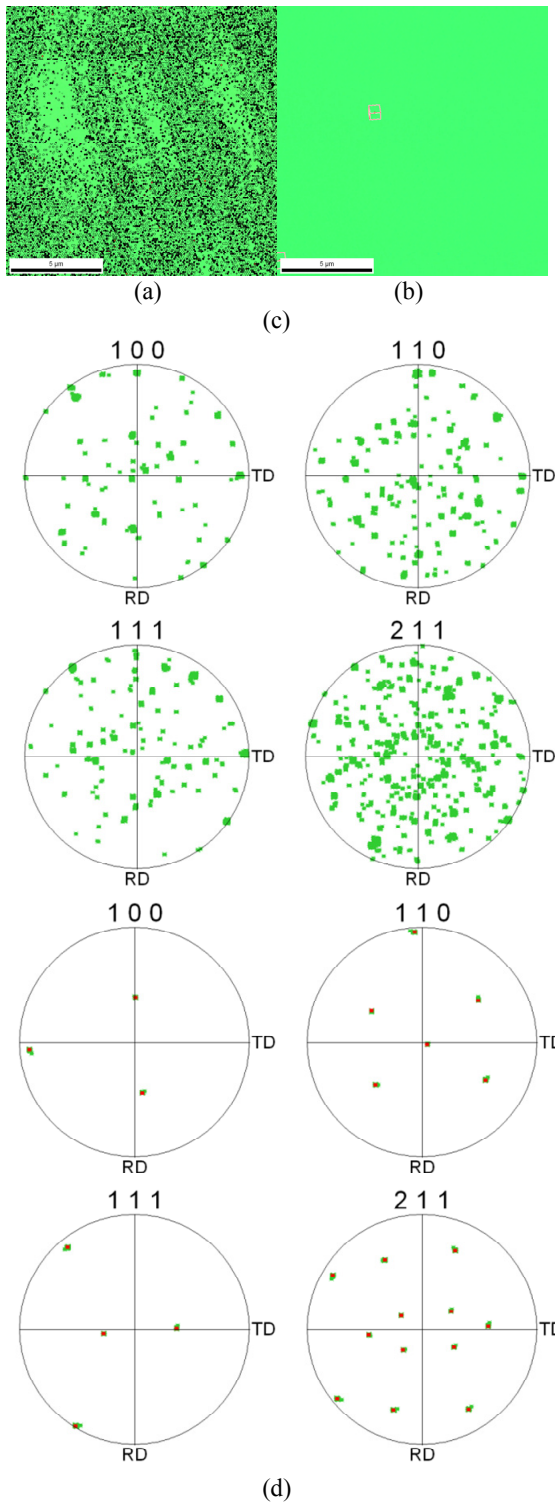


Figure 8: EBSD Map and IPF for two Nb/MgO(110) films coated at 360°C and (a, c) 0V bias and (b, d) -150V bias.

According to Hutchinson *et al* [8-10], epitaxial growth of Nb on MgO(100) has three possible orientations: *O*, *O_p*, and *F*. The strict relationships are presented by Miller

indexes in Table 4 [6] and illustrated in figure 9.

In this study, only the *F*-type orientation has been observed. At high bias voltage (-120V ~ -200V), Nb{110} films exhibit single crystal behavior.

Table 4: Three-dimensional epitaxy relationship of Nb/MgO(100) [Reprint of TABLE I. in ref. 8].

TABLE I. Tabulation of the lattice misfit parameters for the observed orientation (*O*), (001)_{Nb}//(001)_{MgO} with [010]_{Nb}//[010]_{MgO}, a more favored orientation (*F*), (101)_{Nb}//(001)_{MgO} with [011]_{Nb}//[100]_{MgO}, and a second possible orientation *O_p*, (001)_{MgO} with [110]_{Nb}//[010]_{MgO}.

Orientation	Parallel directions	% misfit
<i>O</i>	[100] _{Nb} //[100] _{MgO}	19.4
	[010] _{Nb} //[010] _{MgO}	19.4
<i>O_p</i>	[100] _{Nb} //[010] _{MgO}	8.0
	[100] _{Nb} //[110] _{MgO}	56.5
<i>F</i>	[011] _{Nb} //[100] _{MgO}	8.0
	[010] _{Nb} //[010] _{MgO}	19.4

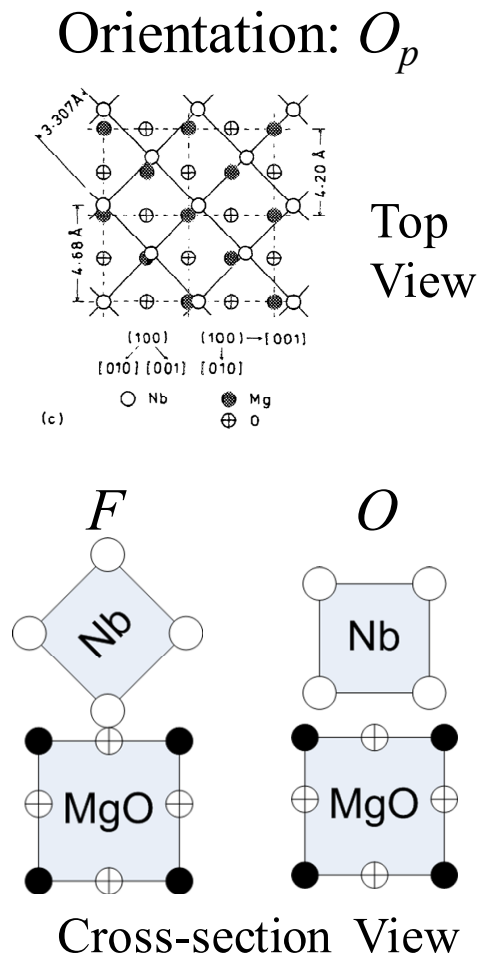


Figure 9: Illustration of three types Nb/MgO(100) epitaxial relationship, as proposed by Hutchinson *et al* [8-10].

SUMMARY

Single-crystal-like Nb films are produced with the JLab ECR Nb plasma ion source on a variety of crystalline substrates, such as *a*-plane and *c*-plane sapphire, and magnesium oxide (100). The films' growth mechanism is hetero-epitaxy. The orientations of the thin films depend strongly on the substrate crystal planes, as well as on the bias voltage i.e. the kinetic energy of the incident Nb⁺ ions. This study reveals such epitaxial relationship as: Nb{110}||Al₂O₃{11-20}, Nb{110}||Al₂O₃{0001}, Nb{111}||Al₂O₃{0001} and Nb{110}||MgO(100).

The substrate heating temperature (about 360°C) to promote epitaxy via ECR coating is moderate, roughly 0.23*T*_{m, Nb}. Our experimental data help to elaborate the roles of ion energy and coating temperature in the Modified Structural Zone Model proposed by Anders [11] recently.

Results of this study are helpful to understand the growth of Nb under different conditions and contribute to the determination of the optimum coating parameters for other coatings, such as niobium on copper substrates.

ACKNOWLEDGEMENT

This research is authored by Jefferson Science Associates, LLC under U.S. DOE Contract No. DOE-AC05-06OR23177, including specific funding via the American Recovery and Reinvestment Act of 2009.

REFERENCES

- [1] A. Gurevich, Appl. Phys. Lett. **88**, 012511 (2006).
- [2] B. D. Cullity, *Elements of X-Ray Diffraction* (1978).
- [3] X. Zhao, A.-M. Valente-Feliciano, C. Xu, R. L. P. Geng, L., C. E. Reece, K. Seo, R. Crooks, M. Krishnan, A. Gerhan, B. Bures, K. W. Elliott, and J. Wright, Journal of Vacuum Science & Technology A **27**, 620-625 (2009).
- [4] A. R. Wildes, J. Mayer, and K. Theis-Brohl, Thin Solid Films **401**, 7-34 (2001).
- [5] J. H. Claassen, S. A. Wolf, S. B. Qadri, and L. D. Jones, Journal of Crystal Growth **81**, 557-561 (1987).
- [6] S. B. Qadri, J. H. Claassen, P. R. Broussard, and S. A. Wolf, Journal of the Less Common Metals **155**, 327-330 (1989).
- [7] T. Wagner, M. Lorenz, and M. Ruhle, Journal of Materials Research **11**, 1255-1264 (1996). Mat. Res. Symp. Proc, Vol. 440, pp.151-156, (1997). T. Wagner, Journal of Materials Research **13**, 693-702 (1998).
- [8] Hutchinson, Journal Applied Physics **36**, 270 (1964).
- [9] T. E. Hutchinson and K. H. Olsen, J. Appl. Phys. **38**, 4933 (1967).
- [10] J. E. Mattson, Eric E. Fullerton, C. H. Sowers, and S. D. Bader, J. Vac. Sci. Technol. A **13**, 276 (1995).
- [11] A. Anders, Thin Solid Films **518**, 4087-4090 (2010).